18. J. A. Arnone III et al., Nature 455, 383–386 (2008).
19. A. Ahlström et al., Science 348, 895–899 (2015).
20. L. Virlouvet, M. Fromm, New Phytol. 205, 596–607 (2015).
21. K. Ogle et al., Ecol. Lett. 18, 221–235 (2015).
22. L. Corcuera, J. J. Camarero, E. Gil-Pelegrín, Trees (Berlin) 18, 83–92 (2004).
23. U. G. Hacke, V. Stiller, J. S. Sperry, J. Pittermann, K. A. McCulloh, Plant Physiol. 125, 779–786 (2001).
24. W. R. L. Anderegg, J. A. Berry, C. B. Field, Trends Plant Sci. 17, 693–700 (2012).
25. W. R. L. Anderegg et al., Glob. Change Biol. 19, 1188–1196 (2013).
26. Y. Zhang et al., J. Geophys. Res. Biogeosci. 118, 148–157.
27. H. D. Grissino-Mayer, H. C. Fritts, Holocene 7, 235–238 (1997).
28. D. A. Clark et al., Ecol. Appl. 11, 356–370 (2001).
29. B. Choat et al., Nature 491, 752–755 (2012).
30. Materials and methods are available as supplementary materials on Science Online.
31. T. J. Brodribb, S. A. McAdam, G. J. Jordan, S. C. Martins, Proc. Natl. Acad. Sci. U.S.A. 111, 14489–14493 (2014).
32. E. Shevliakova et al., Glob. Biogeochem. Cycles 23, GB2022 (2009).
33. K. Shinozaki, K. Yoda, K. Hozumi, T. Kira, Jap. J. Ecol. 14, 97–105 (1964).
34. M. Reichstein et al., Nature 500, 287–295 (2013).
35. T. L. Powell et al., New Phytol. 200, 350–365 (2013).
36. R. Dybzinski, C. Farrior, A. Wolf, P. B. Reich, S. W. Pacala, Am. Nat. 177, 153–166 (2011).
37. C. E. Farrior, R. Dybzinski, S. A. Levin, S. W. Pacala, Am. Nat. 181, 314–330 (2013).
38. S. Saatchi et al., Proc. Natl. Acad. Sci. U.S.A. 110, 565–570 (2013).
39. R. J. W. Brienen et al., Nature 519, 344–348 (2015).

ACKNOWLEDGMENTS

Funding for this research was provided by NSF (grant no. DEB EF-1340270). W.R.L.A. was supported in part by a NOAA Climate and Global Change Postdoctoral Fellowship, administered by the University Corporation for Atmospheric Research. The views and conclusions contained in this document are those of the authors and should not be interpreted as representing the opinions or policies of the funding agencies. All tree-ring data are available at www.ncdc.noaa.gov/data-access/paleoclimatology-data/datasets/tree-ring. We thank all data contributers at the International Tree-Ring Data Bank. All CMIP5 data are available at http://cmip-pcmdi.llnl.gov/cmip5/data_portal.html. We acknowledge the World Climate Research Programme's Working Group on Coupled Modelling, which is responsible for CMIP, and we thank the climate modeling groups (listed in the supplementary materials) for producing and making available their model output. For CMIP, the U.S. Department of Energy's Program for Climate Model Diagnosis and Intercomparison provides coordinating support and led the development of software infrastructure in partnership with the Global Organization for Earth System Science Portals.

SUPPLEMENTARY MATERIALS

www.sciencemag.org/content/349/6247/528/suppl/DC1
Materials and Methods
Figs. S1 to S10
Table S1
References (40–67)

24 March 2015; accepted 3 July 2015
10.1126/science.aab1833

GLOBAL WARMING

Recent hiatus caused by decadal shift in Indo-Pacific heating

Veronica Nieves,[1,2]* Josh K. Willis,[2] William C. Patzert[2]

Recent modeling studies have proposed different scenarios to explain the slowdown in surface temperature warming in the most recent decade. Some of these studies seem to support the idea of internal variability and/or rearrangement of heat between the surface and the ocean interior. Others suggest that radiative forcing might also play a role. Our examination of observational data over the past two decades shows some significant differences when compared to model results from reanalyses and provides the most definitive explanation of how the heat was redistributed. We find that cooling in the top 100-meter layer of the Pacific Ocean was mainly compensated for by warming in the 100- to 300-meter layer of the Indian and Pacific Oceans in the past decade since 2003.

It has been widely established that Earth is absorbing more energy from the Sun than it is radiating back to space (*1*). Furthermore, this has been attributed to anthropogenic greenhouse gases (*2*). Although global surface temperatures have risen over the previous century, several recent papers have documented a slowdown in the rate of surface warming since 2003 (*3*). Most efforts to explain this surface temperature "hiatus" have suggested that it is compensated for by more rapid warming at deeper levels in the ocean in either the Pacific (*3*–*6*) or Atlantic (*7*) Oceans or a combination of the Southern, Atlantic, and Indian Oceans (*8*). More recently, a study pointed out that heat is piling up in the depths of the Indian Ocean (*9*). These studies suggest that the net rate of ocean heat uptake has continued unabated and that the surface hiatus signature is due to an internal rearrangement of heat within the ocean between the surface and some deeper layer of the ocean. This has implications for the net radiative forcing of Earth, because the ocean is the dominant reservoir for storage of excess heat on time scales longer than 1 year, and ocean heat content increases should approximately equal the net radiative imbalance at the top of the atmosphere (*1*). An alternative hypothesis is that approximately half of the surface hiatus is caused by changes in solar and stratospheric aerosol forcing (*10*). In other words, half of the hiatus signal is caused by reduced uptake of heat by the ocean, as opposed to an internal redistribution of heat.

A vigorous debate has grown over this subject, but it has not yet been informed by comprehensive analysis of the available data over the past two decades. We considered both ocean observational data and widely used reanalysis products (that is, numerical simulations constrained by ocean and sometimes atmospheric observations) that span both of the previous decades. A recent study based on Argo data pointed out that net warming continued unabated, despite the exchange of heat between the top 100-m layer and the thermocline on interannual time scales. (*11*). It did not, however, consider the redistribution of heat between these layers on decadal time scales, its geographic distribution, or how it might differ before and after the start of the hiatus in 2003.

Our analysis indicates that during the most recent decade, cooling in the top 100-m layer of the Pacific Ocean is compensated for by warming in the 100- to 300-m layer of the Western Pacific and Indian Oceans, with the largest contribution in the tropics. The Southern Ocean plays a secondary role in warming the 100- to 300-m layer, but this warming has been steady over both of the past decades. The Atlantic Ocean does show a switch from warming to cooling, but its area is so small that it cannot meaningfully contribute to the hiatus signal in surface temperature over the past decade (figs. S1 and S2). Finally, we find little evidence for any change in warming rates below 700 m between the past decade and the previous one—or that the net ocean heat uptake has slowed in the most recent decade.

Observed temperature trends in the oceans were estimated using objectively analyzed subsurface temperature fields from the World Ocean Atlas (WOA) (*12*), Ishii (*13*), and the Scripps Institution of Oceanography (*14*). Simulated temperature trends, based on reanalyses that assimilate ocean data, have also been examined. We compared observed trends with simulated trends from the Simple Ocean Data Assimilation (SODA), National Centers for Environmental Prediction Global Ocean Data Assimilation System (NCEP GODAS), and the latest European Centre for Medium-Range Weather Forecasts ocean reanalysis system 4 (ECMWF ORAS4) (*15*–*17*) (SODA, NCEP, and ECMWF). We considered global and basin-averaged temperature trends for the periods from 1993 to 2002 (the 90s) and from 2003 onward (the 00s). The periods for the past decade are slightly different depending on the product (table S1). Nevertheless, our results are insensitive to the choice of somewhat different time periods. These periods were chosen based on the assumption that the hiatus began in approximately 2003, when there was a small local maximum in the 5-year moving average of global surface

[1]Joint Institute for Regional Earth System Science and Engineering, University of California, Los Angeles, CA, USA. [2]Jet Propulsion Laboratory, California Institute of Technology, Pasadena, CA, USA.
*Corresponding author. E-mail: veronica.nieves@jpl.nasa.gov

temperature (6). Analysis of ocean heat content estimates (as in the supplementary materials) has also been included.

Comparison of the globally averaged temperature change as a function of depth across the water column for each of the past two decades shows substantially less warming in the second decade in the top 100 m (Fig. 1, A and B, where the gray line corresponds to the average of the two observational estimates). Here the hiatus signal is manifested as slight cooling, or a near-zero trend, at the surface. The difference between the warming rates over the two decades (Fig. 1C) shows substantial temperature slowdown in the past decade near the surface for all estimates. The uncertainty shown in Fig. 1 represents one standard error and is an estimate of the uncertainty due to incomplete sampling of the global average (supplementary materials). Instrument biases during this period have been corrected before objective analysis for both the WOA and Ishii products. Remaining uncertainty due to these corrections has been shown to be small (18). The global average surface temperature has been rising since 2003 by +0.001°C/year. Although not zero, it is slower than the century time-scale warming of +0.0064 ± 0.0015°C/year since 1880 (2). The surface warming of the 00s was also substantially slower than that of the 90s, which warmed at a rate of +0.008°C/year (table S1). The average trend difference between the 90s and the 00s indicates decreased warming of –0.007°C/year near the surface (top 10 m) and –0.0005 ± 0.004°C/year in the average over the 10- to 300-m layer (table S1). The fact that the average warming rate over the top 300-m layer did not change between the 90s and the 00s indicates that even on decadal time scales, most of the hiatus-related cooling at the surface is compensated for by warming in the upper 300 m of the ocean.

Because it covers nearly one-third of Earth's surface, it is not surprising to find that surface cooling during the past decade appears to be mainly driven by the Pacific (figs. S1 and S2). A closer look at different basins (figs. S8 to S12) shows that between 2003 and 2012, the most rapid warming in the top 300 m is around the depth of the thermocline (100 to 200 m) in the Indo-Pacific region and, to a lesser extent, the Southern Ocean. This is also clear in the global maps (fig. S6) and the zonal average temperature trends in the upper 300 m (Fig. 2). In addition, this is where the most active redistribution of heat occurs on shorter time scales due to El Nino–Southern Oscillation (11, 14). It is clear from Figs. 1 and 2 as well as figs. S8 to S12 that there is heat compensation between the top 100-m layer and the 100- to 300-m layer in the Pacific, Indian, and to some extent the Southern Ocean.

The clearest depiction of the past decade's hiatus can be seen in a band near the equator (Fig. 3). In the 90s, the Pacific warmed in the thermocline, while the Indian Ocean cooled in the far west. During the 00s, however, the thermocline in the Pacific sank in the west and shoaled in the east, as described by England *et al.* (6), and the tropical Indian Ocean warmed significantly in the thermocline. It is well known that the Indonesian Throughflow and leakage through the Tasman Sea provide pathways for interannual changes in the Pacific to affect the eastern tropical and subtropical Indian Ocean (19, 20). Furthermore, oceanic Rossby waves can carry changes in thermocline depth (and hence heat content) from the Pacific to the Indian Ocean on multidecadal time scales (21). Our analyses suggest that the long-term cooling trend in the tropical and subtropical South Indian Ocean described by Schwarzkopf and Böning (21) reversed during the period of the hiatus, carrying some of the subsurface heat into the Indian Ocean (Figs. 2 and 3 and fig. S6).

It is clear that temperature trends in the North Atlantic Subpolar Gyre switched from warming to cooling in the most recent decade (fig. S6). However, the area of the Atlantic north of 40°N accounts for only 4% of the global ocean. In fact, if the subpolar gyre is masked out, the time series of global surface temperature and the recent hiatus remain virtually unchanged (fig. S2). There is also no clear indication of anomalous heating in the Atlantic Ocean during the 00s at other depths, excluding a meager amount in Ishii's analysis below 1000 m (fig. S12). This suggests that previous work using Ishii's analysis (7) is an incomplete description of the hiatus and its cause.

Analysis of deep hydrographic data in comparison with satellite measurements of sea-level change indicates a contribution of 0.76 mm/year of sea-level rise due to thermal expansion within the layer from 700 to 2000 m (22). Assuming a thermal expansion coefficient of 1.3×10^{-4} °C^{-1} for that layer, this implies an average warming of 0.0045°C/year between the mid-90s and mid-00s and between 700 and 2000 m. Data below 700 m in the pre-Argo era (before 2004) were extremely scarce (14), which can cause objectively mapped estimates to be biased low (23). WOA's pentadal estimate provides an alternative reference value, which should suffer somewhat less bias, because 5 years of data are mapped simultaneously instead of only 1 year. The WOA pentadal estimate shows a heat content increase of 2.4×10^{21} J/year or about 0.0015°C/year (1993–2002 period, 700- to

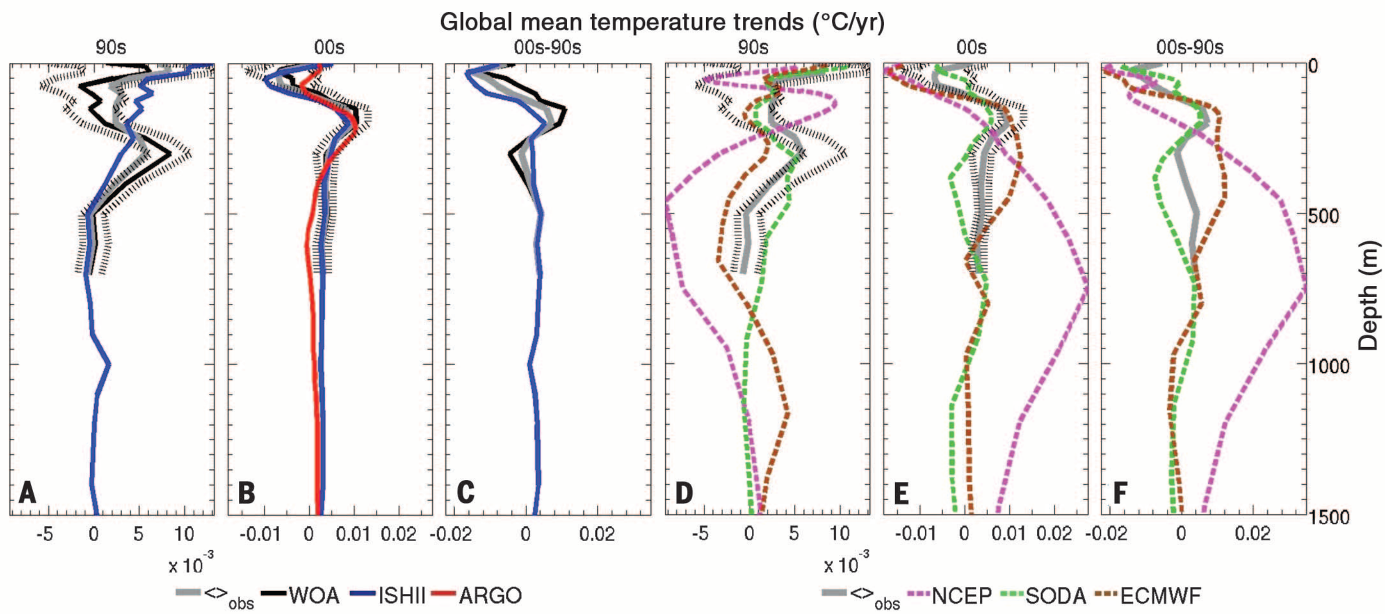

Fig. 1. Global mean temperature trends as a function of depth using observational (**A** to **C**) and model-based (**D** to **F**) products for the 90s [(A) and (D)], 00s [(B) and (E)], and 00s–90s [(C) and (F)]. The gray line corresponds to the average of WOA (black) and Ishii (blue) estimates.

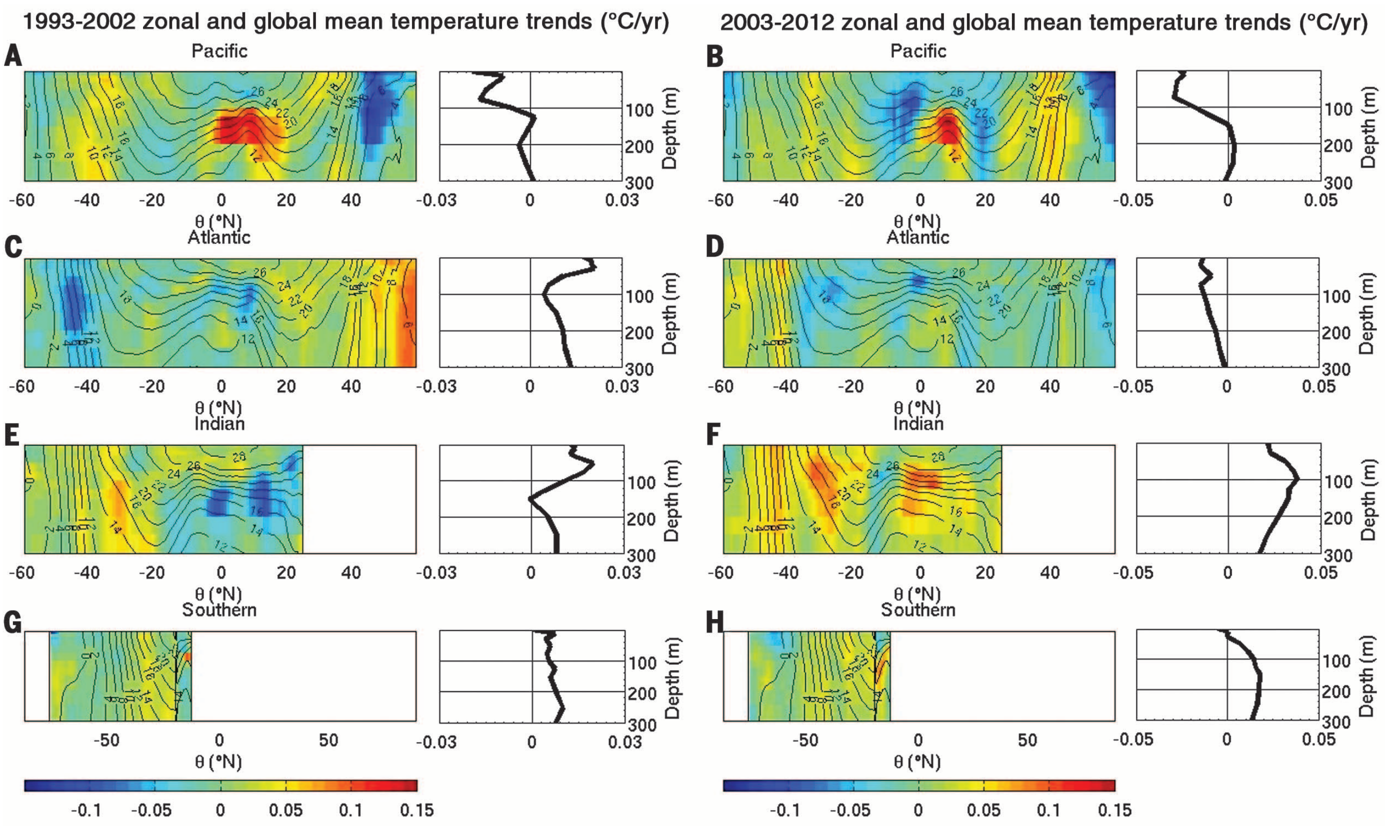

Fig. 2. WOA zonal and global mean temperature trends in the upper 300 m for 1993–2002 (**A**, **C**, **E**, **G**) and 2003–2012 (**B**, **D**, **F**, **H**) and for the Pacific [(A) and (B)], Atlantic [(C) and (D)], Indian [(E) and (F)], and Southern [(G) and (H)] Oceans. Isotherms correspond to the WOA 1955–2013 climatology. For clarity, the Southern Ocean sector is included in the zonal average with each basin (fig. S18). θ (°N), latitude degrees.

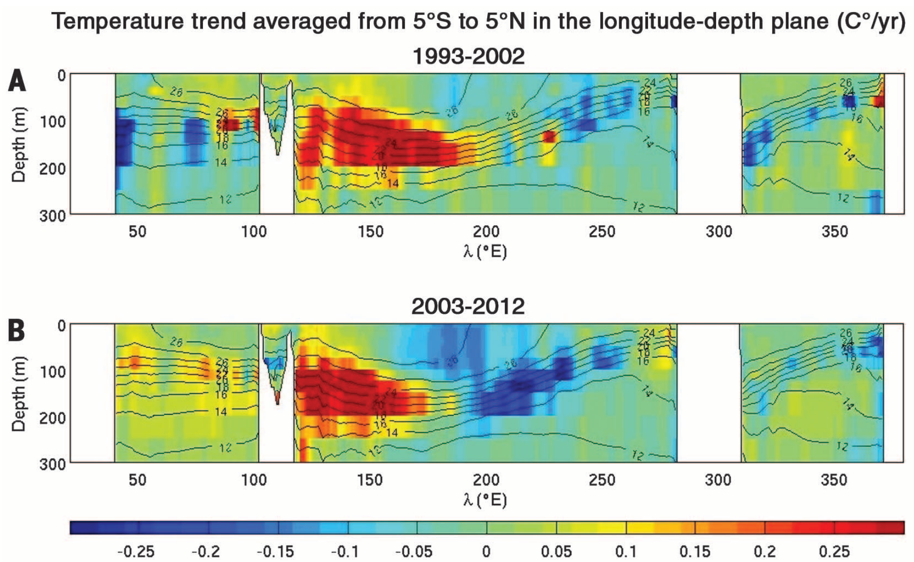

Fig. 3. WOA temperature trends along the equatorial band from 5°S to 5°N in the longitude-depth plane and upper 300 m for 1993–2002 (**A**) and 2003-2012 (**B**). Isotherms correspond to the WOA 1955–2013 climatology. λ (°E), longitude degrees.

2000-m layer). The latter is consistent with the 0.0013°C/year rate of warming for the 700- to 1500-m layer, as measured by the Argo array in the 00s (table S1). Together these findings suggest no significant increase in the rate of warming below 700 m since 2003. This is consistent with Levitus's results (*12*) but contradicts Ishii's estimate, which shows increased heating on the order of +0.0029°C/year between the 90s and the 00s for the same layer (table S1).

Reanalyses also do not seem to correctly reproduce the ocean warming rates, and they lie well outside the observation uncertainty at different depths and times. Both the hiatus and the net amount of heat absorbed by the ocean below 700 m are overestimated (table S1). Reanalyses are also inconsistent with ocean observations, in terms of the vertical and regional distribution of heating. This is true for both global and basin-wide averages (bottom panel of Fig. 1 and figs. S8 to S12). We found that biases are model-dependent, with NCEP showing the largest deviations, followed by ECMWF (particularly in the 00s within the 300- to 700-m layer) and SODA. The NCEP rates of ocean warming clearly show large deviations from the observations at many depths during both decades. There is no observational evidence for such large amounts of warming below the thermocline in the 00s, peaking at 750 m. Nor is there evidence to support such rapid cooling below 2000 m during both decades (fig. S8). Such large signals seem likely to be unphysical and related to some type of uncorrected model drift. The ECMWF model is also problematic. During the 00s, it strongly overestimates the hiatus, and it suggests strong warming between 300 and 700 m, which is much larger than that seen in any observational analysis. This is surprising because

Argo provides excellent coverage of this ocean volume during the 00s, and it shows less than half the amount of warming over these depths (Fig. 1). In contrast, SODA compares well with observational results from WOA and Argo over the top 1000 m. This is expected, given SODA's ocean data assimilation scheme, which nudges the model toward the data without necessarily requiring energy to be conserved in the model domain. During the 00s, however, SODA does show significant cooling between 1000 and 2000 m, which seems contradictory to all observational estimates.

In terms of heat content integrated from the surface down, all reanalyses also show large deviations from observations (fig. S7). Similar results have been found at regional scale (figs. S13 to S17). The observational rate of heat content increase over the 0- to 1500-m depth range did not change significantly between the 90s (2.0×10^{21} J/year) and the 00s (3.4×10^{21} J/year or 2.53×10^{21} J/year, according to the observational average or Argo, respectively) (table S2). Thus, observational heat content estimates do not reveal any obvious hiatus. This suggests that since the early 90s, there has been a steady rate of net ocean heat uptake, and the amount of radiative imbalance at the top of the atmosphere remained practically unchanged between the 90s and the 00s. This contradicts one recent study (*8*) suggesting that the net ocean heat uptake was reduced during the 00s on the basis of changes in surface flux estimates.

Comparison of several of the most commonly used reanalyses with ocean observations raises concerns about their fidelity in simulating temperature changes or in quantitatively explaining the redistribution of heat associated with the recent surface temperature hiatus. Observational estimates provide a more accurate means of assessing oceanic temperature changes and show clear decadal signals that are robust across different analyses (fig. S5) and clearly significant relative to observational errors. Our findings support the idea that the Indo-Pacific interaction in the upper-level water (0 to 300 m depth) regulated global surface temperature over the past two decades and can fully account for the recently observed hiatus. Furthermore, as previously shown for interannual fluctuations (*11*), the decade-long hiatus that began in 2003 is the result of a redistribution of heat within the ocean, rather than a change in the net warming rate.

REFERENCES AND NOTES

1. J. A. Church *et al.*, *Geophys. Res. Lett.* **38**, L18601 (2011).
2. Intergovernmental Panel on Climate Change, in *Climate Change 2013: The Physical Science Basis*, T. F. Stocker *et al.*, Eds. (Cambridge Univ. Press, Cambridge, 2013).
3. Y. Kosaka, S. P. Xie, *Nature* **501**, 403–407 (2013).
4. K. E. Trenberth, J. T. Fasullo, *Earth's Future* **1**, 19–32 (2013).
5. M. A. Balmaseda, K. E. Trenberth, E. Källén, *Geophys. Res. Lett.* **40**, 1754–1759 (2013).
6. M. H. England *et al.*, *Nat. Clim. Change* **4**, 222–227 (2014).
7. X. Chen, K. K. Tung, *Science* **345**, 897–903 (2014).
8. S. S. Drijfhout *et al.*, *Geophys. Res. Lett.* **41**, 7868–7874 (2014).
9. S. K. Lee *et al.*, *Nat. Geosci.* **8**, 445–449 (2015).
10. M. Huber, R. Knutti, *Nat. Geosci.* **7**, 651–656 (2014).
11. D. Roemmich *et al.*, *Nat. Clim. Change* **5**, 240–245 (2015).
12. S. Levitus *et al.*, *Geophys. Res. Lett.* **39**, L10603 (2012).
13. M. Ishii, A. Shouji, S. Sugimoto, T. Matsumoto, *Int. J. Climatol.* **25**, 865–879 (2005).
14. D. Roemmich, J. Gilson, *Geophys. Res. Lett.* **38**, L13606 (2011).
15. T. Nishida, T. Kitakado, H. Matsuura, Validation of the Global Ocean Data Assimilation System (GODAS) data in the NOAA National Centre for Environmental System (NCEP) by theory, comparative studies, applications and sea truth. *IOTC-2011-WPB09-11* (2011).
16. M. A. Balmaseda, K. Mogensen, A. T. Weaver, *Q. J. R. Meteorol. Soc.* **139**, 1132–1161 (2013).
17. J. A. Carton, B. Giese, *Mon. Weather Rev.* **136**, 2999–3017 (2008).
18. L. Cheng, J. Zhu, R. Cowley, T. Boyer, S. Wijffels, *J. Atmos. Ocean. Technol.* **31**, 1793–1825 (2014).
19. J. Sprintall, A. Révelard, *J. Geophys. Res.* **119**, 1161–1175 (2014).
20. E. van Sebille *et al.*, *J. Geophys. Res.* **119**, 1365–1382 (2014).
21. F. U. Schwarzkopf, C. W. Böning, *Geophys. Res. Lett.* **38**, L12602 (2011).
22. S. G. Purkey, G. C. Johnson, D. P. Chambers, *J. Geophys. Res.* **119**, 7509–7522 (2014).
23. J. M. Lyman, G. C. Johnson, *J. Clim.* **21**, 5629–5641 (2008).

ACKNOWLEDGMENTS

The research described in this paper was carried out at the Jet Propulsion Laboratory, California Institute of Technology, under a contract with NASA. This work was supported by grant NNN13D772T-10-OSST10-0015.

SUPPLEMENTARY MATERIALS

www.sciencemag.org/content/349/6247/532/suppl/DC1
Materials and Methods
Figs. S1 to S18
Tables S1 and S2
References (*24*–*30*)

8 December 2014; accepted 24 June 2015
Published online 9 July 2015
10.1126/science.aaa4521

ACTIN-DIRECTED TOXIN

ACD toxin–produced actin oligomers poison formin-controlled actin polymerization

David B. Heisler,[1,2] Elena Kudryashova,[1]† Dmitry O. Grinevich,[1]* Cristian Suarez,[3] Jonathan D. Winkelman,[3] Konstantin G. Birukov,[4] Sainath R. Kotha,[5] Narasimham L. Parinandi,[5] Dimitrios Vavylonis,[6] David R. Kovar,[3,7] Dmitri S. Kudryashov[1,2]†

The actin cross-linking domain (ACD) is an actin-specific toxin produced by several pathogens, including life-threatening spp. of *Vibrio cholerae*, *Vibrio vulnificus*, and *Aeromonas hydrophila*. Actin cross-linking by ACD is thought to lead to slow cytoskeleton failure owing to a gradual sequestration of actin in the form of nonfunctional oligomers. Here, we found that ACD converted cytoplasmic actin into highly toxic oligomers that potently "poisoned" the ability of major actin assembly proteins, formins, to sustain actin polymerization. Thus, ACD can target the most abundant cellular protein by using actin oligomers as secondary toxins to efficiently subvert cellular functions of actin while functioning at very low doses.

Bacterial toxins are the deadliest compounds on the planet. As little as a single molecule of a delivered toxin can compromise vital functions or even kill an affected host cell (*1*, *2*). This is achieved by amplification of a toxin enzymatic activity by signaling cascades (e.g., by cholera, pertussis, and anthrax toxins) or by enzymatic inhibition of vital host complexes present in relatively few copies (e.g., Shiga and diphtheria toxins acting on ribosomes). Such efficiency is crucial because (i) the amount of a toxin produced early after infection is limited by an initially small number of bacterial cells; (ii) the host is protected by commensal bacteria; and (iii) the host immune system efficiently neutralizes toxins by means of adaptive (antibodies) and innate (e.g., defensins) (*3*) humoral defense factors.

Owing to its importance in multiple cellular processes, actin is a common target for bacterium- and parasite-produced toxins. Upon delivery to the cytoplasm of host cells by type I (as part of MARTX toxin) (*4*) or type VI (within VgrG1 toxin) (*5*) secretion systems, the actin cross-linking domain toxin (ACD) catalyzes the covalent cross-linking of Lys^{50} (K50) in subdomain 2 of one actin monomer with Glu^{270} (E270) in subdomain 3 of another actin monomer by means of an amide bond, which results in the formation of actin oligomers (*6*, *7*). The actin subunits in the oligomers are oriented similarly to short-pitch subunits in the filament, except that a major twist of subdomain 2, required to accommodate such orientation, disrupts the normal intersubunit interface and precludes polymerization (*6*).

The currently accepted mechanism of ACD toxicity, by sequestering of bulk amounts of actin as nonfunctional oligomers, is compromised owing to the high concentration of actin (hundreds of micromolar) in a typical animal cell.

Recent hiatus caused by decadal shift in Indo-Pacific heating
Veronica Nieves *et al.*
Science **349**, 532 (2015);
DOI: 10.1126/science.aaa4521